IP_3-dependent, post-tetanic calcium transients induced by electrostimulation of adult skeletal muscle fibers

Mariana Casas,[1] Reinaldo Figueroa,[1,2] Gonzalo Jorquera,[1] Matías Escobar,[1] Jordi Molgó,[3] and Enrique Jaimovich[1]

[1]Centro de Estudios Moleculares de la Célula, ICBM, Facultad de Medicina, Universidad de Chile, Santiago 8380453, Chile
[2]Escuela de Tecnología Médica, Facultad de Medicina, Universidad de Chile, Santiago 8380453, Chile
[3]Institut de Neurobiologie Alfred Fessard, Centre National de la Recherche Scientifique, F-91198 Gif-sur-Yvette cedex, France

Tetanic electrical stimulation induces two separate calcium signals in rat skeletal myotubes, a fast one, dependent on Cav 1.1 or dihydropyridine receptors (DHPRs) and ryanodine receptors and related to contraction, and a slow signal, dependent on DHPR and inositol trisphosphate receptors (IP_3Rs) and related to transcriptional events. We searched for slow calcium signals in adult muscle fibers using isolated adult flexor digitorum brevis fibers from 5–7-wk-old mice, loaded with fluo-3. When stimulated with trains of 0.3-ms pulses at various frequencies, cells responded with a fast calcium signal associated with muscle contraction, followed by a slower signal similar to one previously described in cultured myotubes. Nifedipine inhibited the slow signal more effectively than the fast one, suggesting a role for DHPR in its onset. The IP_3R inhibitors Xestospongin B or C (5 µM) also inhibited it. The amplitude of post-tetanic calcium transients depends on both tetanus frequency and duration, having a maximum at 10–20 Hz. At this stimulation frequency, an increase of the slow isoform of troponin I mRNA was detected, while the fast isoform of this gene was inhibited. All three IP_3R isoforms were present in adult muscle. IP_3R-1 was differentially expressed in different types of muscle fibers, being higher in a subset of fast-type fibers. Interestingly, isolated fibers from the slow soleus muscle did not reveal the slow calcium signal induced by electrical stimulus. These results support the idea that IP_3R-dependent slow calcium signals may be characteristic of distinct types of muscle fibers and may participate in the activation of specific transcriptional programs of slow and fast phenotype.

INTRODUCTION

Ca^{2+} is a ubiquitous intracellular signal that controls an impressive number of cellular processes; this versatility of Ca^{2+} as a second messenger is possible because intracellular Ca^{2+} signals are both spatially and temporally segregated.

In skeletal muscle cells, membrane depolarization induces a conformational change in Cav1.1 dihydropyridine receptors (DHPRs) that is transmitted to the ryanodine receptor (RyR1), causing it to release Ca^{2+} from the sarcoplasmic reticulum. Besides the canonical calcium transient associated with excitation–contraction coupling, calcium waves unrelated to Ca^{2+} spikes involved in excitation–contraction coupling have long been described in chick and rodent myotubes (Flucher and Andrews, 1993; Powell et al., 1996).

Our laboratory has reported the presence of a complex pattern of calcium transients induced by depolarization, related to both excitation–contraction and excitation–transcription signaling in cultured muscle cells. In addition to the fast calcium transient mediated by the RyR channels, which drives muscle contraction, there is an IP_3 receptor (IP_3R)–mediated calcium release that generates long-lasting calcium transients (Jaimovich et al., 2000; Powell et al., 2001). DHPRs act as voltage sensors for this depolarization-evoked slow calcium transient (Araya et al., 2003).

The IP_3-induced calcium signal, which appears most prominently in the nuclei as well as faintly in the cytoplasm surrounding the nuclei, is not related to muscle contraction. We have reported a role for this signal in the regulation of several transcription-related events following membrane depolarization (Carrasco et al., 2003; Juretic et al., 2006, 2007).

In primary culture of rat skeletal muscle cells, high K^+–induced depolarization triggers transient activation of both ERK MAPK and the transcription factor cAMP/Ca^{2+} response element binding protein, as well as an increase in the early genes *c-fos, c-jun*, and *egr-1* mRNAs (Powell et al., 2001; Carrasco et al., 2003). The activation of these transcriptional regulators occurs in the absence of extracellular calcium or in the presence of high

Correspondence to Enrique Jaimovich: ejaimovi@med.uchile.cl

Abbreviations used in this paper: DHPR, dihidropyridine receptors; EDL, extensor digitorium longus; FDB, flexor digitorum brevis; IP_3Rs, inositol trisphosphate receptors; MyHC, myosin heavy chain; NFAT, nuclear factor of activated T cells; RyR, ryanodine receptor; TnIf, fast isoform of Troponin I; TnIs, slow isoform of Troponin I.

The Rockefeller University Press $30.00
J. Gen. Physiol. Vol. 136 No. 4 455–467
www.jgp.org/cgi/doi/10.1085/jgp.200910397

concentrations of ryanodine, which are inhibitory of the RyR response, but is significantly reduced by inhibitors of the IP_3R system that block the generation of the slow calcium transient. Collectively, these results indicate that the slow Ca^{2+} transients mediated by the IP_3R are related to signaling pathways that may be part of the early steps in transcriptional activation of skeletal muscle cells. Although we have extensively characterized this process in cultured muscle cells, these signals have proven difficult to see in adult skeletal muscle fibers.

Different types of muscle fibers exist in adult muscle, varying in both the force and speed of contraction and the fatigue resistance they feature. Each fiber type expresses a characteristic set of contractile proteins and metabolic enzymes that gives them these specific macroscopic features, in agreement with their role in body movements. Muscles that maintain body posture, subjected to low-frequency, repetitive contractions, are composed of mainly slow-twitch oxidative fibers, whereas those involved in fast, nonfrequent movements are mainly composed of fast-twitch glycolytic fibers. Muscle fiber contraction patterns originate from firing patterns of the motoneuron innervating them. Indeed, sustained contractile activity of slow-twitch fibers is the result of a pattern of low-frequency tonic stimulation proper to the electrical activity of those motoneurons. Conversely, the phasic, high-frequency pattern characteristic of fast motoneurons matches with the contractile properties of fast muscle fibers (Burke et al., 1973, 1982; Ausoni et al., 1990; Kernell et al., 1999; Celichowski, 2000).

Nerve activity plays a major role in specification and maintenance of a skeletal muscle fiber's phenotype, which depends on both myoblast lineage and motoneuron innervation (Gunning and Hardeman, 1991; DiMario and Stockdale, 1997; Buckingham, 2001; Kalhovde et al., 2005). The role of motoneuron activity has been demonstrated by different experimental approaches, such as denervation, cross-reinnervation, and external electrostimulation (Foehring et al., 1987, 1988; Hennig and Lomo, 1987; Gorza et al., 1988; Bacou et al., 1996; Roy et al., 1996). Moreover, external electrostimulation with different firing patterns corresponding to different motoneuron subclasses allows the establishment of specific transcriptional programs that control fiber-type identity and growth and can induce a fiber-type transition by inducing expression of specific myosin heavy chains and other contractile proteins as well as metabolic enzymes corresponding to the stimulation pattern used (Pette and Vrbova, 1985; Murgia et al., 2000; Liu et al., 2001; Serrano et al., 2001; Kubis et al., 2002).

Troponin I is a protein of the contractile machinery that possesses two isoforms; these are differentially expressed in distinct muscle fibers types (Banerjee-Basu and Buonanno, 1993), and their regulation is under nerve activity control (Calvo et al., 1996). Expression of the slow isoform of Troponin I (TnIs) is restricted to slow-twitch fibers, whereas fast isoform (TnIf) is restricted to fast-twitch fibers, and both isoforms are down-regulated in denervated muscles. External electrical stimulation of the denervated muscle with a slow pattern (10 Hz) induces a specific up-regulation of the TnIs gene, whereas stimulation with the fast pattern (100 Hz) up-regulates the TnIf isoform (Calvo et al., 1996).

Although some molecular mechanisms involved in differential gene expression induced by motoneuron electrical activity have been described, the mechanisms by which the muscle fiber translates the different firing patterns of motoneurons to induce specific gene transcription programs remain largely unknown. Intracellular Ca^{2+} has been found to be an important second messenger mediating activity-dependent transcription in skeletal muscle. Among transcriptional pathways that can be activated by calcium signals are the calcineurin–nuclear factor of activated T cells (NFAT), Ca^{2+}-calmodulin dependent kinases II and IV, and PKC pathways (Chin et al., 1998; Liu et al., 2001; Serrano et al., 2001; Wu et al., 2002). In innervated avian cultured myotubes, IP_3R-1 is more abundant in fast muscle fibers compared with slow ones. Moreover, inhibition of IP_3R-1 induces a fast to slow fiber-type transition and expression of slow myosin heavy chain 2 gene, in part due to a reduction of NFAT-dependent transcription and nuclear localization, suggesting that IP_3R-1 activity can regulate NFAT transcription factor activity in skeletal muscle fibers and participate in muscle plasticity (Jordan et al., 2005).

We have set up a protocol for culturing slow and fast adult skeletal muscle fibers and have studied calcium transients evoked by field tetanic stimulation of individual fibers using confocal microscopy. We found that fast fibers display an IP_3R-dependent calcium component, which could be involved in regulating the fast to slow fiber phenotype transition.

MATERIALS AND METHODS

Muscle fiber cultures

5–7-wk-old BalbC mice were used in this study. Isolated muscle fibers from mouse flexor digitorum brevis (FDB) and soleus were obtained by enzymatic digestion of the whole muscle with collagenase type 2 (Worthington) (90 min at 450–500 U/ml) and mechanic dissociation with fire-polished Pasteur pipettes, similarly as previously described (Rosenblatt et al., 1995). Isolated fibers were seeded in matrigel-coated coverslips in Dulbecco's modified Eagle medium supplemented with 10% horse serum. Fibers where used 20 h after seeding.

Electrical stimulation and image acquisition

Isolated FDB fibers were incubated 30 min with 5 μM Fluo3-AM at room temperature in standard Krebs physiological solution of the following composition (mM): 140 NaCl, 5 KCl, 1 $CaCl_2$, 1 $MgCl_2$, 5.6 glucose, 10 HEPES-Tris, pH 7.4. Electrical stimulation was applied with a couple of platinum electrodes connected through an isolation unit to a stimulator. Trains of 0.3-ms square pulses with different duration were used in each case. During stimulation

experiments, fibers were in Krebs buffer at 21–23°C. Experiments with no extracellular calcium were in the same Krebs buffer without calcium and supplemented with 0.5 mM EGTA.

Image series during stimulation experiments were obtained with a confocal microscope (Carl Zeiss, Inc. Axiovert 135 M, LSM Microsystems). After excitation with a 488-nm wavelength argon laser, the fluorescence images were collected every 1.0–2.0 s (corresponding to exposure time for each image) and analyzed frame by frame. The average cell fluorescence, F, was calculated for each image on an outline of the cell and normalized to its initial or pre-intervention value F_0 as $(F - F_0)/F_0$. Caution was taken to use minimal laser power in all experiments (a maximum of 10% of maximal laser power). For rapid image acquisitions, data were obtained by line scan of fibers every 1.92 ms; these data were analyzed with the software program WinWCP (J. Dempster, Strathclyde University, Glasgow, Scotland).

Inhibitors

To block DHPR, 25 µM nifedipine was added to the physiological medium for 15 min. To specifically block IP_3Rs, either 5 µM Xestospongin C (XeC) or 5 µM Xestospongin B (XeB) were applied for 20 or 30 min, respectively, to fiber preparations. In the case of nerve muscle preparation, incubation with 20 µM XeB was used. We used XeB or C according to availability. Both toxins have been reported to be effective (Jaimovich et al., 2005), although some variability between batches makes it advisable to test the alternative toxin in case of negative results.

Membrane potential and action potential records

Membrane potential and action potentials were recorded in isolated fibers as described above. Records were made with microelectrodes filled with 1 M potassium glutamate and 20 mM KCl (pH 7.4) with ~40 MΩ tip resistance. An Ag/AgCl electrode in a salt bridge filled with the same solution was used as ground reference. The microelectrode was connected to a Micro-Probe System Model M-707 (WPI). The output was offset corrected, and the capacity was compensated and then digitized by an analogue to digital converter (Labmaster DMA, Scientific Solutions).

Immunofluorescence

Cryosections (10–14 µm thick) from adult mice muscles were fixed using freshly prepared para-formaldehyde (2–4%) for 15 min, washed 3 times with 0.1 M PBS, pH 7.4, and blocked with PBS containing 2% BSA for 1 h. Incubation with specific primary antibodies were made in the same blockade buffer at 4°C overnight. Next, muscle sections were washed in PBS and incubated with Alexa-conjugated secondary antibody for 1 h at room temperature and finally mounted with Vectashield (Vector Laboratories, Inc.). Mounted sections were examined by confocal microscopy. Representative images were acquired with a Carl Zeiss, Inc. Axiovert 135 microscope (LSM Microsystems).

Antibodies to a purified epitope of type-1 IP_3R were provided by M. Estrada (Universidad de Chile, Santiago, Chile). Antibodies recognizing type-2 and type-3 IP_3R were from Chemicon. Antibodies directed against fast and slow myosin heavy chains were obtained from Sigma-Aldrich. Antibodies directed against fast IIX and IIA myosin heavy chains were provided by P. Maire (Institut Cochin, Paris, France). Alexa 488 and Alexa 633–conjugated anti-rabbit or anti-mouse immunoglobulin G were from Molecular Probes.

Nerve muscle preparation

The nerve muscle preparation was made from a mouse extensor digitorium longus (EDL) muscle as previously reported for diaphragm (Minic et al., 2003). The muscle was dissected keeping tendons at both extremities and keeping the axons innervating it. After loading for 30 min with Fluo3-AM, the muscle was fixed by its tendons in a holder chamber and the nerve was stimulated with 600 ms train duration (150-µs pulse duration) at 20 Hz. The muscle was kept in oxygenated Krebs physiological solution. Imaging was performed with a multiphoton scanning confocal microscope LSM 510 META (Carl Zeiss, Inc.), mounted on an upright microscope and controlled through the manufacturer-supplied software and workstation. Images were collected using a water-immersion lens (Plan-Apochromat 20x/1.0). Fluo3AM was excited with the 488-nm wavelength line of an argon ion laser, and Alexa 594 with the 561-nm wavelength line of a DPSS laser. The pinhole aperture was set to 1 Airy Unit. Images were digitized at 12-bit resolution for time lapse into a 512 × 512 pixel array. Data were treated using the manufacturer's software Zen2008. Fluorescence images were collected every 1.57 s and analyzed frame by frame. Images from each experiment were processed identically before quantization by outlining the cell's fluorescence and determining the mean fluorescence before (F_0) and during various treatments (F). The relative fluorescence ($\Delta F/F_0$) was calculated as $(F - F_0)/F_0$.

Real-time PCR

Total RNA from skeletal muscle fiber cultures was obtained using Trizol reagent (Invitrogen) according to manufacturer's protocol. cDNA was prepared by reverse transcription of 1 µg of total RNA, using SuperScript (Invitrogen) according to manufacturer's protocol. Real-time PCR was performed using a Stratagene Mx3000P as follows. The reaction mixture consisted of 2 µl buffer PCR 10X, 0.2 µl platinum Taq DNA polymerase 5 U/µl, 0.6 µl $MgCl_2$ 50 mM, 1 µl sense primer 10 pmol/µl, 1 µl antisense primer 10 pmol/µl, 0.4 µl dNTPs 10X, 2 µl SYBR(R) Green Nucleic A (1/2000), and 1 µl cDNA. The final volume of the mixture was adjusted to 20 µl with the addition of DNase- and RNase-free H_2O. Platinum Taq DNA polymerase and SYBR(R) Green Nucleic A were from Invitrogen.

The primers used were: TnIs: 5′-GAGGTTGTGGGCTTGCTGTATGA-3′ (sense), 5′-GGAGCGCATATTAGGGATGT-3′ (antisense) (Juretic et al., 2007); TnIf: 5′-AGGTGAAGGTGCAGAAGAGC-3′ (sense), 5′-TTGCCCCTCAGGTCAAATAG-3′ (antisense) (Barthel and Liu, 2008); β-actin: 5′-TCTACAATGAGCTGCGTGTG-3′ (sense), 5′-TACATGGCTGGGGTGTTGAA-3′ (antisense).

PCR amplification of the housekeeping gene β-actin was performed as a control. Thermocycling conditions were as follow: 95°C for 2 min and 44 cycles (TnI) or 40 cycles (β-actin) of 95°C for 30 s, 58°C for 30 s, 72°C for 30 s, and 84°C for 7 s, and a final cycle of 7 s at 72°C. PCR products were resolved by electrophoresis on 2% agarose gel and stained with ethidium bromide. Quantification of mRNAs was based on quantity of nanograms. Results were expressed as nanograms TnI/nanograms β-actin ratio (percentage of control).

Data analysis

Results of *n* experiments are expressed as a mean ± SEM, and the significance of differences was evaluated using Student's *t* test for paired data and one-way ANOVA followed by Dunnett's post-test for multiple comparison or Tukey's post-test for multiple pair comparisons. $P < 0.05$ was considered to be statistically significant.

RESULTS

Electrical stimuli induced a two-component Ca^{2+} signal in adult skeletal muscle fibers

When isolated FDB fibers were stimulated with 270 pulses (0.3 ms each) at 45 Hz, we observed that the Ca^{2+} transient had at least two components. The first component was fast, simultaneous to tetanic-pulse stimulation and related to contraction (Fig. 1). A later, slower signal

was observed as a delayed return to basal fluorescence levels after tetanic stimuli. The post-tetanic decay of the calcium signal can be fitted by a two-exponential function, with time constants (at slow sampling rates) τ_1 = 2.26 ± 0.06 s and τ_2 = 18.02 ± 0.45 s (n = 6 fibers, from three independent experiments). The amplitudes of the signal were A_1 = 2.123 ± 0.119 (in arbitrary units) for the fast component and A_2 = 0.473 ± 0.060 for the slow component, the latter representing 18% of the total signal. The second signal has an intracellular origin, because stimulation in the absence of extracellular calcium did not change the signal kinetics (Fig. 1). The slow component of the Ca^{2+} transient is only apparent after tetanus; the Ca^{2+} transient for a single twitch can be fitted by a single exponential decay as seen in the example in Fig. 1 D. In this case, the time constant (at fast sampling rates) is τ = 44.29 ± 2.67 ms (n = 7). After a short tetanus (600 ms, 45 Hz), the slow Ca^{2+} component is barely apparent, but the post-tetanic Ca^{2+} transient can still be fitted by a double exponential decay with time constant τ_1 = 56.22 ± 1.96 ms and τ_2 = 1419.97 ± 278.07 ms (n = 3) (Fig. 1 D). No changes in resting membrane potential were evident after tetanic stimulation; the initial resting membrane potential was 55 ± 1.1 mV and after tetanus was 52.7 ± 2.7 mV (n = 3), all action potentials show a clear overshoot, and action potential half-wide duration was in a range of 1.1–1.6 ms. As post-tetanic after depolarization was not seen, it is not possible to ascribe slow calcium transients to late voltage sensor activity.

As in cultured myotubes, DHPR acts as a membrane potential sensor for the onset of the slow signal. When adult fibers were incubated with 25 μM nifedipine, the slow signal component was abolished. Fast signal amplitude was still present but significantly diminished in

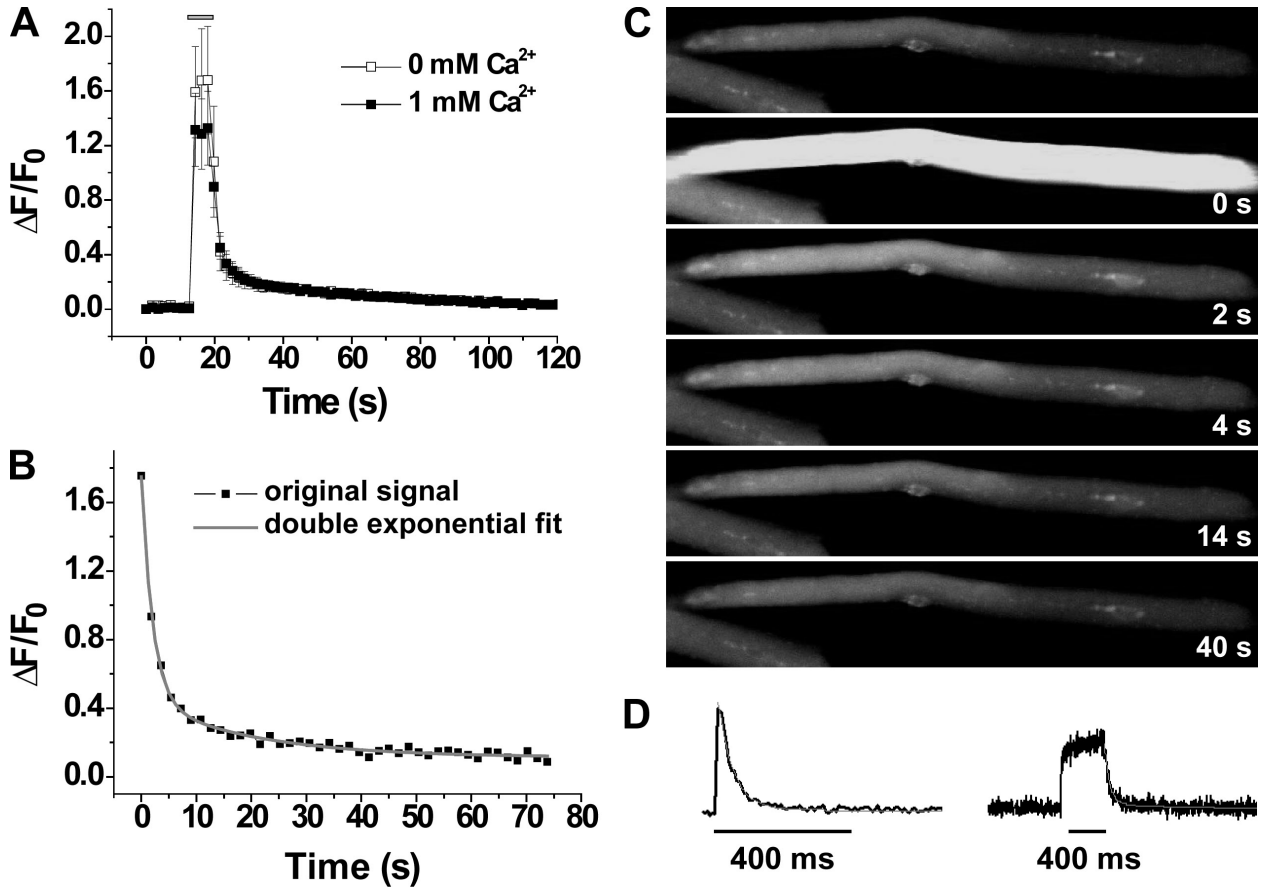

Figure 1. Electrical stimuli induce a two-component Ca^{2+} signal in adult skeletal muscle fibers. Isolated muscle fibers from mouse FDB and loaded with Fluo3-AM were stimulated with a train of 270 pulses (0.3 ms each) at 45 Hz. Images were obtained by confocal microscopy. (A) We observed a first fast Ca^{2+} signal related to contraction when tetanic train was applied (gray bar in the graph) followed by a slower signal, observed as a delayed return to basal fluorescence levels after tetanic stimulus. Experiments were done in the presence of standard Krebs solution containing 1 mM calcium (filled squares, n = 11) or in absence of calcium with a medium supplemented with 0.5 mM EGTA (empty squares, n = 8). Experimental points could be fitted by a double exponential function as shown for a typical record in the lower graph (B). Images on the right (C) correspond to fiber fluorescence before, during, and after application of electrical stimulus (end of stimulation indicated by time = 0 s). (D) Single twitch can be fitted by a single exponential decay as shown for a representative record at left. On the right, an example of the signal obtained after stimulation with a short tetanus (45 Hz, 600 ms). Because of the small number of pulses, the slow signal is barely apparent, although the post-tetanic Ca^{2+} decay can still be fitted by a double exponential.

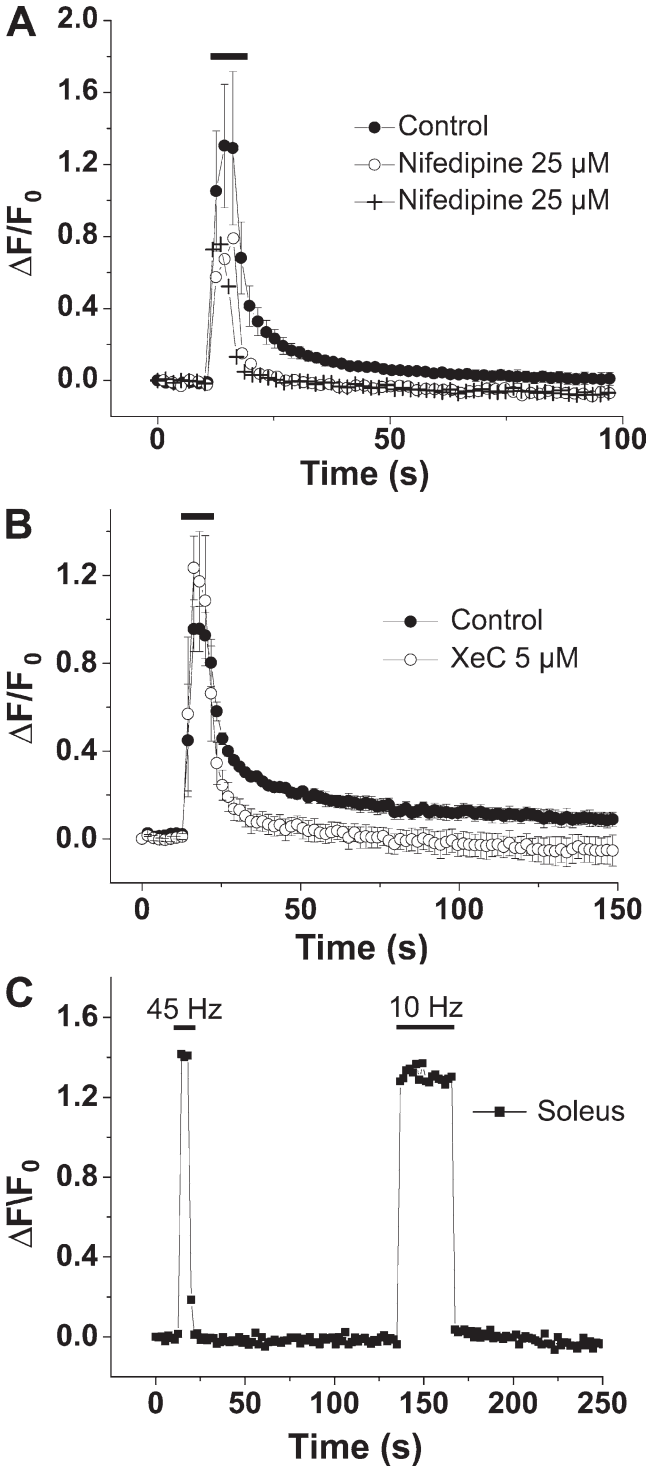

Figure 2. The slow Ca^{2+} signal induced by electrical stimuli is dependent on DHPR and mediated by IP_3, and is not present in isolated fibers of the slow skeletal muscle soleus. Isolated muscle fibers from mouse FDB were obtained and treated as in Fig. 1, loaded with Fluo3-AM, and stimulated with a train of 270 pulses of 0.3 ms each at 45 Hz. (A) 25 μM Nifedipine completely inhibited the slow Ca^{2+} signal induced by a train of 270 pulses, 0.3 ms each at 45 Hz. Full symbols show the mean of control Ca^{2+} signals ($n = 4$). Empty symbols correspond to signals obtained after 15 min of fiber incubation with 25 μM Nifedipine (two representative signals shown in the graph from $n = 4$). (B) Incubation of fibers with 5 μM XeC (empty symbols, $n = 4$), which specifically blocks the Ca^{2+} release by IP_3R, inhibited the slow Ca^{2+} signal induced by electrical stimulation in adult muscle fibers (full symbols, $n = 4$). These experiments were done in the presence of 1 mM extracellular Ca^{2+}. (C) Isolated muscle fibers from soleus were obtained and seeded by a method similar to that for FDB. Fibers were then stimulated with 270 pulses of 0.3 ms each at 45 and 10 Hz. Figure shows a representative signal (from $n = 6$). We observe no delayed return to basal levels, the signals resembling those of FDB fibers in the presence of inhibitors of the slow Ca^{2+} signal, indicating the absence of this slow Ca^{2+} signal in soleus fibers.

these conditions (Fig. 2 A). Incubation of fibers with 5 μM XeC, which specifically blocks the Ca^{2+} release by IP_3R, also inhibited the slow Ca^{2+} signal induced by electrical stimulation in adult muscle fibers (Fig. 2 B). Fitting of post-tetanic Ca^{2+} signals from fibers preincubated with XeC show an 80% reduction in τ_2 value, with no effect in τ_1 value. If we wanted to report these results in terms of changes in amplitude values, we would use the values of tau obtained for control experiments, and in this case the fitted amplitude of the slow calcium transient drops to <0.1% of the total signal.

The slow Ca^{2+} signal is not present in isolated fibers of the slow skeletal muscle soleus

We wanted to know whether the slow Ca^{2+} signal found in FDB fibers would be present in soleus muscle fibers. Isolated muscle fibers from soleus were obtained and seeded using a procedure similar to that used for FDB. Fibers were then stimulated with 270 pulses of 0.3 ms each at 45 and 10 Hz. Representative transients for these fibers can be observed in Fig. 2 C. No delayed return to basal levels was observed, and these signals were closer to those obtained in FDB fibers treated with inhibitors for the slow Ca^{2+} signal, suggesting the absence of this slow signal in soleus fibers.

The slow Ca^{2+} signal is dependent on frequency and duration of the electrical stimulus

To evaluate the role of frequency and duration of stimulus on slow Ca^{2+} signal features, we stimulated fibers at 2, 5, 10, 45, and 90 Hz. To compare the effect of train duration, we chose a 45-Hz frequency, and we stimulated with 23, 68, and 270 pulses. To eliminate fiber to fiber amplitude signal variations, the same fiber was stimulated with three successive trains at 2, 5, and 10 Hz, with intervals of 100 s between them. In another set of fibers, the sequence was inverted (i.e., 10, 5, and 2 Hz) to avoid a possible bias due to successive train stimulations. The same type of protocol was performed at higher frequencies, with successive trains of 10, 45, and 90 Hz. The 10-Hz amplitude value was used as reference point to compare amplitudes at all frequencies studied and the values obtained for different sets of fibers (in the two frequency's orders for each series) were processed together. Ca^{2+} signal

amplitude was evaluated as the area under the $\Delta F/F_0$ curve, in the time window between 4 and 60 s after the stimulus end. We choose 4 s as the time to start measuring slow signal amplitude because at this time the fast signal was already negligible (as seen in experiments using slow signal inhibitors). Alternatively, the post-tetanic Ca^{2+} signals recorded from fibers stimulated at 2, 10, and 90 Hz were fitted to double exponential decay, considering tau values obtained for control signals at 45 Hz ($\tau_1 = 2.26$ s and $\tau_2 = 18$ s). Fast signal was arbitrarily normalized to a constant value, and the values obtained for amplitudes for fast and slow components showed that slow component represents 66.45 ± 10.57% of total signal at 10 Hz, whereas for 2 and 90 Hz, this value drops to 35.37 ± 8.86% and 37.57 ± 2.85%, respectively. The values for 2 and 90 Hz are significantly different from that obtained at 10 Hz, with $P < 0.05$. If we normalize by the 10-Hz value, we observe that at 2 Hz, the slow component corresponds to 53% of the 10-Hz value, whereas at 90 Hz, the slow component represents 57% of this value. This is consistent with the analysis of areas shown in Fig. 3 A. As area calculation gave the same information as amplitudes from fitted signals, we used only area analysis in Fig. 3 B. As a control, we measured the slow calcium signal amplitude in three successive trains at the same frequency (45 Hz) and we found no significant variations (unpublished data).

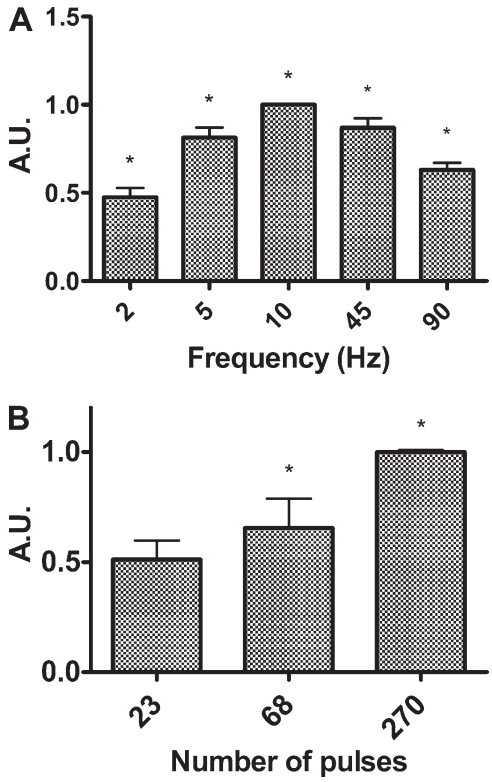

Figure 3. The slow Ca^{2+} signal is dependent on frequency and duration of the electrical stimulus. (A) Individual isolated FDB fibers were stimulated with 270 pulses at 2, 5, and 10 Hz or at 10, 45, and 90 Hz (and in the inverted sequence 10, 5, and 2 Hz and 90, 45, 10 Hz). The magnitude of the slow Ca^{2+} signal was measured as the area under the curve in the post-tetanic region. The values are arbitrary units normalized against the area corresponding to 10 Hz. The graph shows the mean area of different fibers stimulated in both sequences of stimulation frequency. We observe a bell-shaped curve, depending on frequency, with a maximum at 10 Hz. Differences between each pair of frequencies, for each frequency series (i.e., 2 vs. 5, 2 vs. 10, and 5 vs. 10; 10 vs. 45, 10 vs. 90, and 45 vs. 90), are statistically significant (*, $P < 0.05$). (B) The magnitude of slow signal was dependent on the duration of electrical stimuli. The graph shows the mean values for different fibers stimulated at 45 Hz with 23, 68, and 270 pulses. The area values are arbitrary units normalized against signal corresponding to 270 pulses. We observe that the signal magnitude increases with the increase in the stimulus duration. (*, $P < 0.05$)

Interestingly (Fig. 3 A), the amplitude of slow calcium signal showed a bell-shaped curve depending on stimulation frequency. At low frequencies (2 Hz), the calcium signal was much reduced. The amplitude grew to reach a maximum value at frequencies from 10 to 20 Hz. Further increasing the frequency of stimulation produced a decrease in the slow signal amplitude (Fig. 3 A). The number of pulses in the stimulation train also had an impact on the slow signal amplitude, augmenting with an increase in the number of pulses (Fig. 3 B).

Slow Ca^{2+} signal in muscle fibers indirectly stimulated through the motor nerve

Ca^{2+} signals are very difficult to record in neuromuscular preparations due to microscope limitations and to important movement artifacts inherent to contraction during experiments. Nevertheless, this type of preparation was useful because muscle cells are in a more physiological condition, and the stimulation by the nerve is the very source of depolarization of the muscle fiber in vivo.

We were able to make a nerve muscle preparation from a mouse EDL muscle and record the Ca^{2+} signals obtained after stimulation of its nerve. After loading with Fluo3-AM, the muscle was fixed by its tendons in a holder chamber and the nerve was stimulated with 600-ms trains (150 μs of pulse duration) at 20 Hz (Fig. 4). This short train duration was chosen to limit the movement of the preparation to keep the recorded set of fibers in the microscope field. After nerve stimulation, we observed the fast Ca^{2+} signal related to contraction (the movement artifact being evident), and after the contraction finished, a second component very similar to that described in this work for isolated fibers was obtained. Similar to results obtained for isolated fibers, this post-tetanic Ca^{2+} signal can be fitted to a double exponential decay, with time constants $\tau_1 = 2.74 \pm 0.27$ s and $\tau_2 = 13.22 \pm 1.49$ s. As observed in the graph in Fig. 4, this second component was completely abolished when muscle was incubated with 20 μM XeB for 30 min. In this case, post-tetanic signal can be fitted

by a single exponential decay with a time constant $\tau = 1.86$ s.

IP_3R-2 and 3 are expressed in adult muscle at different intracellular locations

All three IP_3R isoforms were expressed in adult muscle. To look for specific locations of each subtype of IP_3R, we made cryosections of different mouse muscles, and the specific expression of each IP_3R isoform was revealed by immunofluorescence (Fig. 5, A–F). IP_3R-2 appears to be expressed in all muscle fibers (only one example is shown) both in scattered clusters at the core of the fiber and in the perinuclear regions (Fig. 5 B, arrows). IP_3R-3 was also expressed in all muscle fibers (one example shown) and seemed to be absent in most of the nuclear regions. It appears to be expressed in a striated pattern, typical for sarcoplasmic reticulum proteins (Fig. 5 A).

IP_3R-1 is absent in slow-type muscle fibers and is expressed preferentially in fast, IIX-type muscle fibers

Unlike IP_3R-2 and -3, IP_3R-1 was not expressed uniformly in all muscle fibers. We observed a mosaic pattern of expression of this IP_3R subtype in all muscles studied (Fig. 5, C–F). To identify the fiber types positively reacting to anti IP_3R-1, we labeled serial sections with antibodies directed against isoforms of myosin heavy chain (MyHC). MyHC I will label type I (slow) fibers, MyHC II will label all type II (fast) fibers, MyHC IIA will label a subtype (IIA) of fast fibers, and MyHC IIX will label all type II fibers except for those type IIX. In soleus sections (Fig. 5, G–I), we observed that IP_3R-1 was absent in type I slow fibers (indicated by asterisks), being expressed only in type II fibers. In tibialis anterior sections, a mainly fast muscle that does not contain slow, type I fibers, the mosaic pattern of expression was also observed

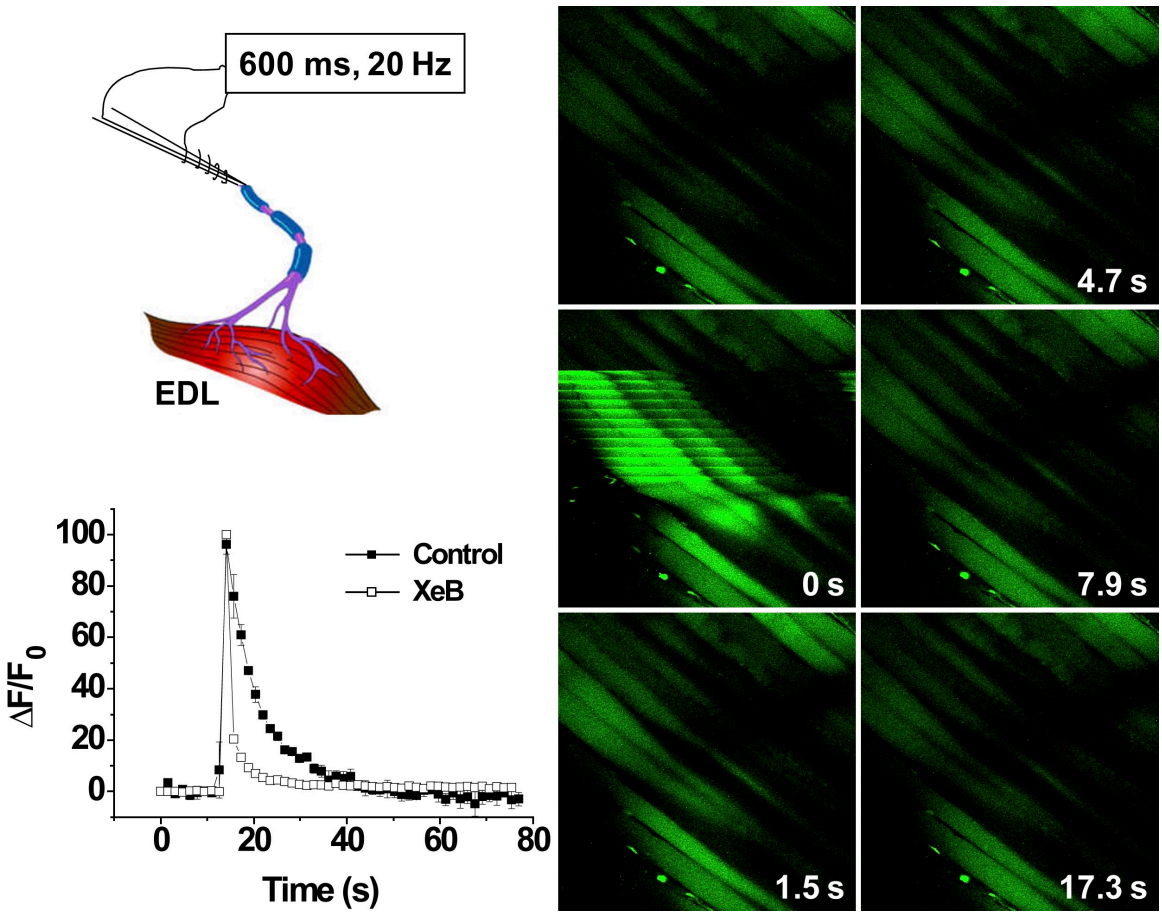

Figure 4. Slow Ca^{2+} signal is observed in muscle fibers directly stimulated by the nerve. A nerve muscle preparation of an EDL muscle was loaded with Fluo3 -AM. The stimulation was performed by a pipette directly trough the nerve as illustrated in the schema (top left). In the right panel, we can see the fluorescence images of the muscle before, during, and after the stimulation through its nerve at 20 Hz for 600 ms. Application of the stimulus is indicated by time = 0 s. Each photograph had a scanning time of 1.57 s with no delay between them. We can see that after the end of tetanus, the fibers took several seconds to return to basal fluorescence levels as in the case for isolated fibers. In the graph at left, the average of four Ca^{2+} signals (filled squares) and the inhibition of the slow component obtained after incubation of nerve muscle preparation for 30 min with 20 μM of XeB (empty squares) are shown. The relative fluorescence levels are normalized to the maximum value obtained for each case.

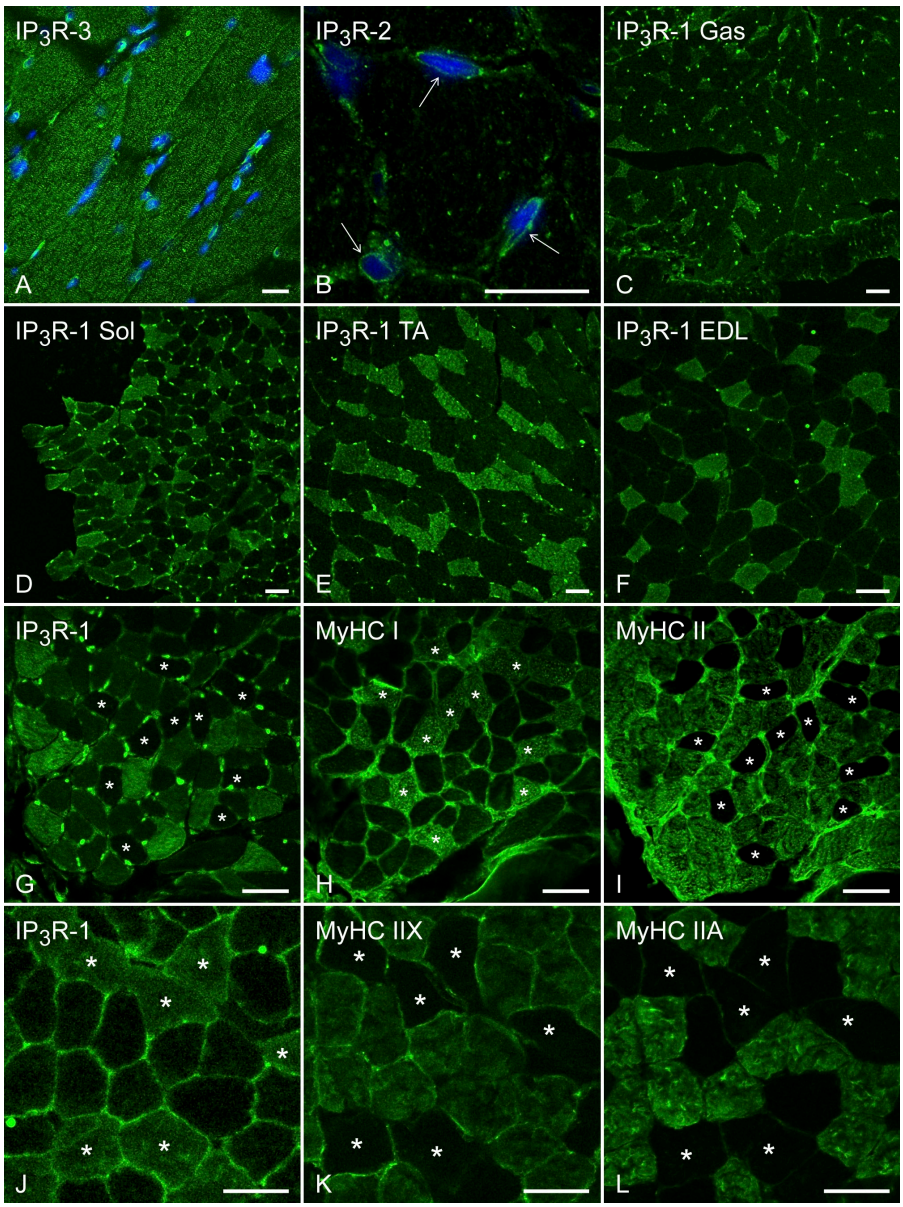

Figure 5. IP_3Rs subtypes are expressed in adult muscle at different intracellular locations. Immunofluorescence images for IP_3Rs and myosin heavy chain markers in different muscle slices are shown. IP_3R-3 was expressed in all muscle fiber types (A) and seems to be absent of most of the nuclear regions. It appears to be expressed in a striated pattern typical for sarcoplasmic reticulum proteins. IP_3R-2 also appears to be expressed in all muscle fibers and is expressed in some clusters at the core of the fiber and in the perinuclear regions (B, arrows). On the other hand, IP_3R-1 is not present in all muscle fibers, showing a mosaic expression pattern in all muscles studied: gastrocnemius (Gas), soleus, tibialis anterior (TA), and EDL (C–F). Immunofluorescence on serial cryosections of adult soleus mouse muscles using antibodies against type 1 IP_3R (G and J), slow MyHC-I (H), MyHC-II (I), MyHC-IIX (labeling all fibers except IIX, panel K), and MyHC-IIA (L). We observe that IP_3R -1 was absent in slow-type fibers, and its expression was restricted to a subgroup of fast fibers, corresponding to type IIX.

(Fig. 5 E), indicating that IP_3R-1 is preferentially expressed in a subset of fast, type II fibers. Using specific antibodies recognizing different type II myosin heavy chains we observed that expression of IP_3R-1 was indeed absent in slow fibers (Fig. 5, G–I) and was limited to fast, mixed metabolism type IIX fibers (Fig. 5, J–L), not stained by an antibody recognizing type IIA fibers nor by that recognizing all fibers but IIX.

IP_3-dependent calcium signal had opposite effects in the expression of slow and fast isoforms of Troponin I gene in adult muscle fibers

We searched for participation of the slow Ca^{2+} signal in transcriptional events in adult fibers and we found that after 45-Hz tetanus stimulation, there was a significant increase of mRNA levels of skeletal troponin I, slow isoform (TnIs), 4 h after the stimulus (Fig. 6 A). TnIs expression levels are in accordance with the variation of slow calcium signal amplitude with frequency of stimulation, as stimulation at 20 Hz (where slow signal has a maximum) induced a higher and sooner increase of TnIs mRNA than 45-Hz stimulation (Fig. 6 A). This increase is dependent on IP_3R because when we blocked them with a specific inhibitor such as XeB before the stimulus, we could no longer observe an increase in TnIs mRNA levels (Fig. 6 B). This result indicates that the slow Ca^{2+} signal participates in transcription activation of the slow isoform of TnI gene.

Importantly, the same stimulus produced a decrease in mRNA of the TnIf, 2 (not depicted) and 4 h poststimulus, that was also inhibited by XeB. This decrease was not observed at 45 Hz (Fig. 6 C).

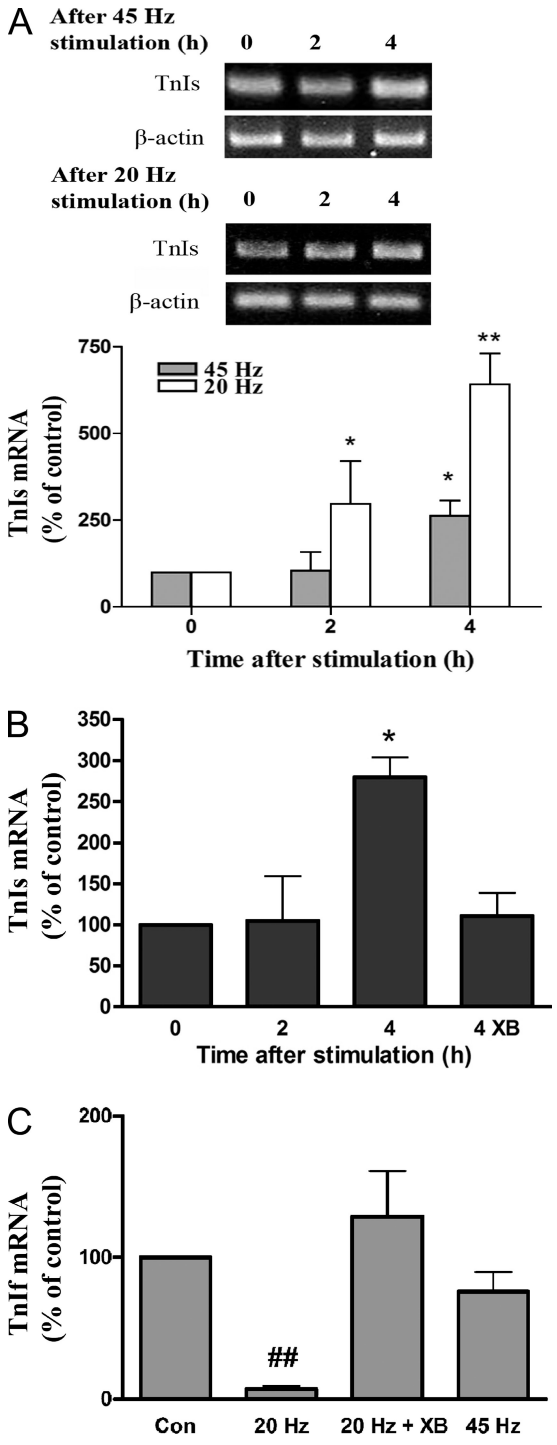

Figure 6. Electrical stimulation induced an IP_3-dependent Troponin I-slow up-regulation and Troponin I-fast down-regulation in a frequency-dependent manner. Isolated muscle fibers from mouse FDB were obtained as in Fig. 1 and stimulated with a train of 270 pulses of 0.3 ms each at 45 Hz or 20 Hz. RNA was extracted at different times post-stimulation and cDNA obtained by RT-PCR. A set of fibers was incubated with 5 μM XeB for 30 min before stimulation (B and C). PCR was performed with primers specific for skeletal TnIs, TnIf, and β-actin, which serves to normalize TnI values. (A). We observe a significant increase of mRNA levels of TnIs two and 4 h after the stimulus (*, $P < 0.05$; **, $P < 0.01$); this increase was much larger for 20 Hz than for 45-Hz stimulation. The increase was not obtained (B) after 4 h when fibers were incubated with the specific inhibitor of IP_3R XeB. (C). TnIf significantly decreased (##, $P < 0.01$) 4 h after 20-Hz stimulus; 45-Hz stimulus shows no effect. The decrease was not obtained after 4 h when fibers were incubated with XeB.

DISCUSSION

In cultured skeletal muscle cells, a mechanism for excitation–transcription coupling, linking electrical activity to gene expression has been described. This mechanism is triggered by Cav1.1 (dihydropyridine receptors) acting as voltage sensors and includes activation of G protein–coupled receptors, PI3 kinase, phospholipase C, and IP_3Rs, a characteristic feature being the presence of a slow, low-intensity calcium transient, unrelated to muscle contraction (Jaimovich et al., 2000; Powell et al., 2001; Araya et al., 2003; Eltit et al., 2006; Buvinic et al., 2009).

In this work we have characterized the Ca^{2+} signals in electrically stimulated adult skeletal muscle fibers. We have shown that in some fibers, two signals are apparent; one is related to contraction during the time duration of electrical stimulus and a second one, observed as a delayed return to basal fluorescence levels after the end of electrical stimuli, is dependent on IP_3R. As expected for a signal with more than one component (see below), the post-tetanic decay can be fitted by a two-exponential function, giving two distinct time constants. The slower one ($\tau = 18.02$ s), can be associated with the IP_3-dependent signal, whereas the fast one may be related to the fast Ca^{2+} release through the EC coupling mechanisms.

The time constant for the fast component cannot be calculated in frame to frame records, the time lapse between frames being too long (1.8 s). To estimate this time constant, we performed line scan in both single twitch and short tetanus experiments. We found values for the fast time constant similar to those reported in the literature (Carroll et al., 1995, 1997; Liu et al., 1997; Capote et al., 2005; Calderon et al., 2009), considering that we have used a relatively high-affinity calcium dye.

The slow component ($\tau = 18$ s) of the calcium transient has not been previously reported in mammalian muscle. Most of the works in the literature deal with single twitch or trains with few pulses at high frequencies (Carroll et al., 1995, 1997) or low affinity dyes (Capote et al., 2005; Calderon et al., 2009), conditions in which the slow component is hard to see; nevertheless, after short tetanus we can still fit a double exponential decay to the post-tetanic Ca^{2+} transient with time constants very similar to those reported recently by Calderon et al. (2010).

It has been demonstrated that the time course of calcium release can be calculated by modeling the decay phase and integrating it in the balance equation for intracellular calcium as described in Melzer et al. (1984, 1987) (see also Delbono and Stefani, 1993; Ursu et al., 2004;

Royer et al., 2008). This model assumed that the rates of calcium removal after the depolarizing stimulus (obtained for experimental data) are the same as those occurring during the depolarization. This implies that the removal systems have the same properties before and after the stimulus. Another assumption is that the calcium release drops rapidly after the end of the stimulus, so modeling the decay phase is equivalent to model the removal process. A slow component of decay was reported in frog muscle (Klein et al., 1991) for decay of fura 2 signals after a 200-ms voltage-clamp depolarization. The authors' interpretation was that this slow decay was consistent with the properties of the calcium extrusion and buffering mechanisms based on a model that considers a single release process, constant calcium leak from sarcoplasmic reticulum, and the sarcoplasmic-endoplasmic reticulum calcium pump acting in a highly cooperative way. We cannot completely rule out the presence of such a component, but these conditions are unlikely to be found in mammalian fibers where parvalbumin levels have been reported to be relatively low (Heizmann et al., 1982) and sarcoplasmic-endoplasmic reticulum calcium pump cooperativity is close to two (Zafar et al., 2008).

In this work, using a similar theoretical approach, we assumed a single exponential decay for initial calcium removal and we fitted the decay phase of the calcium transient to exponential functions as an approximation to evaluate the events occurring in the calcium release process. As in the method described above, we assume that the removal systems have the same properties before and after the stimulus and that the release is finished rapidly after the end of pulses. In this way, decay kinetics can give us information about the release process, even if we do not try to explicitly calculate the rate of calcium release as is done elsewhere (Melzer et al., 1984, 1987; Delbono and Stefani, 1993; Royer et al., 2008).

The fact that the calcium decay after a train of pulses in adult FDB muscle fibers fits to a double exponential decay can be interpreted as follows. First, from the balance equations we can assume that the release process would also have at least two components. Second, as we propose, these two components correspond to calcium fluxes through RyR and IP_3R, and that calcium release through IP_3R has a delay over the calcium released through RyR; it is possible then that part of the calcium release (corresponding to our slow signal) continues after the end of the stimulus. In this case, we could not adopt the second assumption exposed above and the decay phase would represent both the removal process and this late release. In previous works (Melzer et al., 1984; Delbono and Stefani, 1993), the decay phase was fitted to a single exponential decay. This fact has been used as an argument to support the assumption of the stop of release process shortly after the stimulus (Delbono and Stefani, 1993). Using the same argument, the fact that the decay phase in our experiments adjusts to a double exponential decay would indicate the presence of a second and late release event, taking place during and after the end of stimulus.

At a fixed frequency, the amplitude of this second signal is dependent on the number of electrical stimulation pulses, being higher when the number of pulses is increased. This result is coherent with the idea proposed by Eltit et al. (2004) of a dose response–like phenomenon, where the effect on the DHPR as voltage sensor could be additive. In that work, the need of a minimum threshold number of depolarizing events to induce the IP_3-dependent Ca^{2+} signal is also pointed out. Unlike primary myotubes, where this threshold is found at around 200 pulses (at 45 Hz), in adult fibers this threshold appears to be much lower, as the slow Ca^{2+} signal is still visible after 23 stimulation pulses. A possible explanation could be the higher level of organization of membrane structures in the adult muscle cell, which could result in a more efficient signal transduction from the voltage sensor to the IP_3 machinery.

The slow Ca^{2+} signal shows a bell shaped curve as a function of the frequency of stimulation, with a maximum between 10 and 20 Hz. These data suggest that there is a balance between the rate of IP_3 production at the plasma membrane and the rate of activation of IP_3R at the sarcoplasmic reticulum. Activation of DHPR at each pulse could produce a quantum of IP_3, but there could be a need for a minimum number of these quanta to reach the concentration required for activation of IP_3R. Under this hypothesis, at very low frequencies, the rate of IP_3 production (and/or degradation) would not allow the necessary accumulation of this molecule to activate IP_3R. At higher frequencies, accumulation could take place, and the slow signal would appear and increase with frequency until maximal production was reached. To explain the behavior at even higher frequencies, we can hypothesize that there is a maximal frequency that can be detected by the system, limited by the rate of IP_3 synthesis and/or the rate of signal transmission from DHPR to IP_3 production machinery. At these high frequencies, the machinery would not be able to detect the stimulus or sustain an increasing production. The time lapse of IP_3 production and consequently the duration of the slow calcium signal would be a function of the duration of the stimulation train at a given frequency; by keeping the number of pulses constant, the actual duration of the tetanic stimulus diminishes and so does the magnitude of the Ca^{2+} signal as shown in Fig. 3 A.

We found no slow Ca^{2+} signal in fibers from soleus muscle, even if IP_3R-2 and 3 are expressed in this muscle and approximately half of its fibers also express IP_3R-1. Coincidentally, Calderon et al. (2010) have recently reported two time constants decay for fast

muscle fibers and only one for slow-type fibers. Talon et al. (1999) measured the IP_3-evoked Ca^{2+} signals in permeabilized muscle fibers from soleus and EDL (a fast type) mouse muscles. They found that in both muscles, IP_3 produces Ca^{2+} release from the sarcoplasmic reticulum that yields a measurable contracture of the muscle. The amplitude of this contracture was larger in soleus than in EDL muscle, confirming the fact that IP_3 participates in Ca^{2+} release in adult skeletal muscle. Nevertheless, that experiment only shows the presence of functional IP_3R in adult muscle, but does not link the production of IP_3 to a physiological membrane stimulus. Our results in soleus muscle could be explained by a lack of link between depolarization events and the PLC activation that leads to IP_3 production. In this sense, a previous report from Mayr and Thieleczek (1991) shows that in fast and mixed-type muscle from *Xenopus leavis* and in mixed-type rat gastrocnemius muscle, there is an increase of IP_3 concentration after tetanic stimulation. Interestingly, they do not see such increase in the slow soleus muscle under the same tetanic stimulus. This report supports our speculation that the signaling protein complex (Buvinic et al., 2009) that links DHPR to PLC activation and IP_3 production may be absent or not functional in soleus muscle.

Another line of explanation comes from the fact that soleus is a muscle with oxidative metabolism and a high mitochondria content. The calcium-buffering role of mitochondria has been well demonstrated in different cell types as well as in muscle (Isaeva and Shirokova, 2003; Isaeva et al., 2005). It would be possible that soleus does have IP_3-dependent signals, but the mitochondria content, and then its buffering capacity, is high enough to prevent its visualization. Experiments of stimulation in the presence of mitochondrial uncoupling drugs could be useful to assess this point.

We have shown that IP_3-dependent signals are also present in muscle fibers directly stimulated by the nerve. This reinforces the idea that slow calcium signals are indeed physiologically relevant for muscle function. In a previous work from our laboratory, it was shown that slow signals were present in the neuromuscular region on a hemi-diaphragm preparation when stimulated with high extracellular potassium (Powell et al., 2003). The present work extends this result, demonstrating that slow signals are present in the whole muscle fiber when stimulated with a physiological activity pattern.

All three types of IP_3Rs are expressed in adult skeletal muscle. The particular expression pattern of each one could reflect a differential participation in the slow Ca^{2+} signal generation, as seen before for other IP_3-dependent Ca^{2+} signals (Iino, 2000; Hernandez et al., 2007). The perinuclear expression of IP_3R-2 could preferentially mediate nuclear signals, whereas IP_3R-3 could participate more in cytoplasmic signals. In the case of IP_3R-1, the differential expression between distinct fiber types suggests the presence of a mechanism that represses its expression in slow-type fibers. It is possible that IP_3R-1 transcription could be sensitive to muscle activity pattern (i.e., frequency and load), as is the case for other genes whose expression is restricted to specific fiber types, like myosin heavy chains or some metabolic enzymes (Ausoni et al., 1990; Schiaffino et al., 1999; Pette and Staron, 2001). Transcription of IP_3R-1 has been reported to increase in cultured muscle cells upon electrical stimulation (Valdes et al., 2008) or by innervation (Jordan et al., 2005). Further experiments must be done to probe the effect of different stimulation patterns on IP_3R-1 transcription. On the other hand, the differential presence of IP_3R-1 in different muscle fiber types could involve the generation of specific calcium signals in those fibers where it is expressed, having a role in the plasticity of fiber phenotype. Experiments of knock-down of IP_3R-1 in adult muscle will help us to elucidate this point.

The slow Ca^{2+} signal has a role in transcription activation of several genes in cultured myotubes (Juretic et al., 2007). In adult muscle, we have shown that mRNA of slow TnI is increased after electrical stimulation whereas expression of the fast isoform of TnI was repressed by the same stimulus. Both induction of TnIs at low frequencies and repression of TnIf at high frequencies are IP_3R dependent as they were inhibited by XeB. It is interesting to note that TnIs is a gene expressed only in slow fiber types and its transcription is under control of neural activity (Calvo et al., 1996; Rana et al., 2005). As mentioned, we have seen that slow Ca^{2+} signals are sensitive to frequency and duration of the electrical stimulus. We can speculate that in adult muscle, slow Ca^{2+} signals act as a decoding tool of different stimulation patterns incoming from the motor neuron, which participate in muscle plasticity. The fact that slow Ca^{2+} signals were not present in slow muscle fibers and the fact that they participate in regulation of slow-type genes in fast fibers would suggest that the slow Ca^{2+} signal is involved in the induction of a slow phenotype, mediated by a particular pattern of electrical stimulation of fast muscle fibers.

We want to thank Jorge Hidalgo and Paola Llanos for their help in measuring membrane potential in isolated fibers.

This work was financed by Fondo Nacional de Ciencia y Tecnología (FONDECYT) 1080120, Fondo Nacional de Areas Prioritarias (FONDAP) 15010006, PBC 24, and Centre National de la Recherche Scientifique-Conicyt. M. Casas was financed by PBC24 Bicentennial Academic Insertion Program.

Edward N. Pugh Jr. served as editor.

Submitted: 31 December 2009
Accepted: 13 August 2010

REFERENCES

Araya, R., J.L. Liberona, J.C. Cardenas, N. Riveros, M. Estrada, J.A. Powell, M.A. Carrasco, and E. Jaimovich. 2003. Dihydropyridine receptors as voltage sensors for a depolarization-evoked, IP3R-mediated, slow calcium signal in skeletal muscle cells. *J. Gen. Physiol.* 121:3–16. doi:10.1085/jgp.20028671

Ausoni, S., L. Gorza, S. Schiaffino, K. Gundersen, and T. Lomo. 1990. Expression of myosin heavy chain isoforms in stimulated fast and slow rat muscles. *J. Neurosci.* 10:153–160.

Bacou, F., P. Rouanet, C. Barjot, C. Janmot, P. Vigneron, and A. d'Albis. 1996. Expression of myosin isoforms in denervated, cross-reinnervated, and electrically stimulated rabbit muscles. *Eur. J. Biochem.* 236:539–547. doi:10.1111/j.1432-1033.1996.00539.x

Banerjee-Basu, S., and A. Buonanno. 1993. Cis-acting sequences of the rat troponin I slow gene confer tissue- and development-specific transcription in cultured muscle cells as well as fiber type specificity in transgenic mice. *Mol. Cell. Biol.* 13:7019–7028.

Barthel, K.K., and X. Liu. 2008. A transcriptional enhancer from the coding region of ADAMTS5. *PLoS One.* 3:e2184. doi:10.1371/journal.pone.0002184

Buckingham, M. 2001. Skeletal muscle formation in vertebrates. *Curr. Opin. Genet. Dev.* 11:440–448. doi:10.1016/S0959-437X(00)00215-X

Burke, R.E., D.N. Levine, P. Tsairis, and F.E. Zajac III. 1973. Physiological types and histochemical profiles in motor units of the cat gastrocnemius. *J. Physiol.* 234:723–748.

Burke, R.E., R.P. Dum, J.W. Fleshman, L.L. Glenn, A. Lev-Tov, M.J. O'Donovan, and M.J. Pinter. 1982. A HRP study of the relation between cell size and motor unit type in cat ankle extensor motoneurons. *J. Comp. Neurol.* 209:17–28. doi:10.1002/cne.902090103

Buvinic, S., G. Almarza, M. Bustamante, M. Casas, J. Lopez, M. Riquelme, J.C. Saez, J.P. Huidobro-Toro, and E. Jaimovich. 2009. ATP released by electrical stimuli elicits calcium transients in skeletal muscle. *J. Biol. Chem.* 284:34490–34505. doi:10.1074/jbc.M109.057315

Calderon, J.C., P. Bolanos, S.H. Torres, G. Rodriguez-Arroyo, and C. Caputo. 2009. Different fibre populations distinguished by their calcium transient characteristics in enzymatically dissociated murine flexor digitorum brevis and soleus muscles. *J. Muscle Res. Cell Motil.* 30:125–137. doi:10.1007/s10974-009-9181-1

Calderon, J.C., P. Bolanos, and C. Caputo. 2010. Myosin heavy chain isoform composition and Ca(2+) transients in fibres from enzymatically dissociated murine soleus and extensor digitorum longus muscles. *J. Physiol.* 588:267–279. doi:10.1113/jphysiol.2009.180893

Calvo, S., J. Stauffer, M. Nakayama, and A. Buonanno. 1996. Transcriptional control of muscle plasticity: differential regulation of troponin I genes by electrical activity. *Dev. Genet.* 19:169–181. doi:10.1002/(SICI)1520-6408(1996)19:2<169::AID-DVG9>3.0.CO;2-7

Capote, J., P. Bolanos, R.P. Schuhmeier, W. Melzer, and C. Caputo. 2005. Calcium transients in developing mouse skeletal muscle fibres. *J. Physiol.* 564:451–464. doi:10.1113/jphysiol.2004.081034

Carrasco, M.A., N. Riveros, J. Rios, M. Muller, F. Torres, J. Pineda, S. Lantadilla, and E. Jaimovich. 2003. Depolarization-induced slow calcium transients activate early genes in skeletal muscle cells. *Am. J. Physiol. Cell Physiol.* 284:C1438–C1447.

Carroll, S.L., M.G. Klein, and M.F. Schneider. 1995. Calcium transients in intact rat skeletal muscle fibers in agarose gel. *Am. J. Physiol.* 269:C28–C34.

Carroll, S.L., M.G. Klein, and M.F. Schneider. 1997. Decay of calcium transients after electrical stimulation in rat fast- and slow-twitch skeletal muscle fibres. *J. Physiol.* 501:573–588. doi:10.1111/j.1469-7793.1997.573bm.x

Celichowski, J. 2000. Mechanisms underlying the regulation of motor unit contraction in the skeletal muscle. *J. Physiol. Pharmacol.* 51:17–33.

Chin, E.R., E.N. Olson, J.A. Richardson, Q. Yang, C. Humphries, J.M. Shelton, H. Wu, W. Zhu, R. Bassel-Duby, and R.S. Williams. 1998. A calcineurin-dependent transcriptional pathway controls skeletal muscle fiber type. *Genes Dev.* 12:2499–2509. doi:10.1101/gad.12.16.2499

Delbono, O., and E. Stefani. 1993. Calcium transients in single mammalian skeletal muscle fibres. *J. Physiol.* 463:689–707.

DiMario, J.X., and F.E. Stockdale. 1997. Both myoblast lineage and innervation determine fiber type and are required for expression of the slow myosin heavy chain 2 gene. *Dev. Biol.* 188:167–180. doi:10.1006/dbio.1997.8619

Eltit, J.M., J. Hidalgo, J.L. Liberona, and E. Jaimovich. 2004. Slow calcium signals after tetanic electrical stimulation in skeletal myotubes. *Biophys. J.* 86:3042–3051. doi:10.1016/S0006-3495(04)74353-2

Eltit, J.M., A.A. Garcia, J. Hidalgo, J.L. Liberona, M. Chiong, S. Lavandero, E. Maldonado, and E. Jaimovich. 2006. Membrane electrical activity elicits inositol 1,4,5-trisphosphate-dependent slow Ca2+ signals through a Gbetagamma/phosphatidylinositol 3-kinase gamma pathway in skeletal myotubes. *J. Biol. Chem.* 281:12143–12154. doi:10.1074/jbc.M511218200

Flucher, B.E., and S.B. Andrews. 1993. Characterization of spontaneous and action potential-induced calcium transients in developing myotubes in vitro. *Cell Motil. Cytoskeleton.* 25:143–157. doi:10.1002/cm.970250204

Foehring, R.C., G.W. Sypert, and J.B. Munson. 1987. Motor-unit properties following cross-reinnervation of cat lateral gastrocnemius and soleus muscles with medial gastrocnemius nerve. I. Influence of motoneurons on muscle. *J. Neurophysiol.* 57:1210–1226.

Foehring, R.C., G.W. Sypert, and J.B. Munson. 1988. Relation of whole muscle contractile properties to source of innervation. *Exp. Neurol.* 101:366–373. doi:10.1016/0014-4886(88)90048-9

Gorza, L., K. Gundersen, T. Lomo, S. Schiaffino, and R.H. Westgaard. 1988. Slow-to-fast transformation of denervated soleus muscles by chronic high-frequency stimulation in the rat. *J. Physiol.* 402:627–649.

Gunning, P., and E. Hardeman. 1991. Multiple mechanisms regulate muscle fiber diversity. *FASEB J.* 5:3064–3070.

Heizmann, C.W., M.W. Berchtold, and A.M. Rowlerson. 1982. Correlation of parvalbumin concentration with relaxation speed in mammalian muscles. *Proc. Natl. Acad. Sci. USA.* 79:7243–7247. doi:10.1073/pnas.79.23.7243

Hennig, R., and T. Lomo. 1987. Effects of chronic stimulation on the size and speed of long-term denervated and innervated rat fast and slow skeletal muscles. *Acta Physiol. Scand.* 130:115–131. doi:10.1111/j.1748-1716.1987.tb08118.x

Hernandez, E., M.F. Leite, M.T. Guerra, E.A. Kruglov, O. Bruna-Romero, M.A. Rodrigues, D.A. Gomes, F.J. Giordano, J.A. Dranoff, and M.H. Nathanson. 2007. The spatial distribution of inositol 1,4,5-trisphosphate receptor isoforms shapes Ca2+ waves. *J. Biol. Chem.* 282:10057–10067. doi:10.1074/jbc.M700746200

Iino, M. 2000. Molecular basis of spatio-temporal dynamics in inositol 1,4,5-trisphosphate-mediated Ca2+ signalling. *Jpn. J. Pharmacol.* 82:15–20. doi:10.1254/jjp.82.15

Isaeva, E.V., and N. Shirokova. 2003. Metabolic regulation of Ca2+ release in permeabilized mammalian skeletal muscle fibres. *J. Physiol.* 547:453–462. doi:10.1113/jphysiol.2002.036129

Isaeva, E.V., V.M. Shkryl, and N. Shirokova. 2005. Mitochondrial redox state and Ca2+ sparks in permeabilized mammalian skeletal muscle. *J. Physiol.* 565:855–872. doi:10.1113/jphysiol.2005.086280

Jaimovich, E., R. Reyes, J.L. Liberona, and J.A. Powell. 2000. IP(3) receptors, IP(3) transients, and nucleus-associated Ca(2+) signals in cultured skeletal muscle. *Am. J. Physiol. Cell Physiol.* 278:C998–C1010.

Jaimovich, E., C. Mattei, J.L. Liberona, C. Cardenas, M. Estrada, J. Barbier, C. Debitus, D. Laurent, and J. Molgo. 2005. Xestospongin B, a competitive inhibitor of IP3-mediated Ca2+ signalling in

cultured rat myotubes, isolated myonuclei, and neuroblastoma (NG108-15) cells. *FEBS Lett.* 579:2051–2057. doi:10.1016/j.febslet.2005.02.053

Jordan, T., H. Jiang, H. Li, and J.X. DiMario. 2005. Regulation of skeletal muscle fiber type and slow myosin heavy chain 2 gene expression by inositol trisphosphate receptor 1. *J. Cell Sci.* 118:2295–2302. doi:10.1242/jcs.02341

Juretic, N., P. Garcia-Huidobro, J.A. Iturrieta, E. Jaimovich, and N. Riveros. 2006. Depolarization-induced slow Ca2+ transients stimulate transcription of IL-6 gene in skeletal muscle cells. *Am. J. Physiol. Cell Physiol.* 290:C1428–C1436. doi:10.1152/ajpcell.00449.2005

Juretic, N., U. Urzua, D.J. Munroe, E. Jaimovich, and N. Riveros. 2007. Differential gene expression in skeletal muscle cells after membrane depolarization. *J. Cell. Physiol.* 210:819–830. doi:10.1002/jcp.20902

Kalhovde, J.M., R. Jerkovic, I. Sefland, C. Cordonnier, E. Calabria, S. Schiaffino, and T. Lomo. 2005. "Fast" and "slow" muscle fibres in hindlimb muscles of adult rats regenerate from intrinsically different satellite cells. *J. Physiol.* 562:847–857. doi:10.1113/jphysiol.2004.073684

Kernell, D., R. Bakels, and J.C. Copray. 1999. Discharge properties of motoneurones: how are they matched to the properties and use of their muscle units? *J. Physiol. (Paris).* 93:87–96. doi:10.1016/S0928-4257(99)80139-9

Klein, M.G., L. Kovacs, B.J. Simon, and M.F. Schneider. 1991. Decline of myoplasmic Ca2+, recovery of calcium release and sarcoplasmic Ca2+ pump properties in frog skeletal muscle. *J. Physiol.* 441:639–671.

Kubis, H.P., R.J. Scheibe, J.D. Meissner, G. Hornung, and G. Gros. 2002. Fast-to-slow transformation and nuclear import/export kinetics of the transcription factor NFATc1 during electrostimulation of rabbit muscle cells in culture. *J. Physiol.* 541:835–847. doi:10.1113/jphysiol.2002.017574

Liu, Y., S.L. Carroll, M.G. Klein, and M.F. Schneider. 1997. Calcium transients and calcium homeostasis in adult mouse fast-twitch skeletal muscle fibers in culture. *Am. J. Physiol.* 272:C1919–C1927.

Liu, Y., Z. Cseresnyes, W.R. Randall, and M.F. Schneider. 2001. Activity-dependent nuclear translocation and intranuclear distribution of NFATc in adult skeletal muscle fibers. *J. Cell Biol.* 155:27–39. doi:10.1083/jcb.200103020

Mayr, G.W., and R. Thieleczek. 1991. Masses of inositol phosphates in resting and tetanically stimulated vertebrate skeletal muscles. *Biochem. J.* 280:631–640.

Melzer, W., E. Rios, and M.F. Schneider. 1984. Time course of calcium release and removal in skeletal muscle fibers. *Biophys. J.* 45:637–641. doi:10.1016/S0006-3495(84)84203-4

Melzer, W., E. Rios, and M.F. Schneider. 1987. A general procedure for determining the rate of calcium release from the sarcoplasmic reticulum in skeletal muscle fibers. *Biophys. J.* 51:849–863. doi:10.1016/S0006-3495(87)83413-6

Minic, J., A. Chatonnet, E. Krejci, and J. Molgo. 2003. Butyrylcholinesterase and acetylcholinesterase activity and quantal transmitter release at normal and acetylcholinesterase knockout mouse neuromuscular junctions. *Br. J. Pharmacol.* 138:177–187. doi:10.1038/sj.bjp.0705010

Murgia, M., A.L. Serrano, E. Calabria, G. Pallafacchina, T. Lomo, and S. Schiaffino. 2000. Ras is involved in nerve-activity-dependent regulation of muscle genes. *Nat. Cell Biol.* 2:142–147. doi:10.1038/35004013

Pette, D., and R.S. Staron. 2001. Transitions of muscle fiber phenotypic profiles. *Histochem. Cell Biol.* 115:359–372.

Pette, D., and G. Vrbova. 1985. Neural control of phenotypic expression in mammalian muscle fibers. *Muscle Nerve.* 8:676–689. doi:10.1002/mus.880080810

Powell, J.A., L. Petherbridge, and B.E. Flucher. 1996. Formation of triads without the dihydropyridine receptor alpha subunits in cell lines from dysgenic skeletal muscle. *J. Cell Biol.* 134:375–387. doi:10.1083/jcb.134.2.375

Powell, J.A., M.A. Carrasco, D.S. Adams, B. Drouet, J. Rios, M. Muller, M. Estrada, and E. Jaimovich. 2001. IP(3) receptor function and localization in myotubes: an unexplored Ca(2+) signaling pathway in skeletal muscle. *J. Cell Sci.* 114:3673–3683.

Powell, J.A., J. Molgo, D.S. Adams, C. Colasante, A. Williams, M. Bohlen, and E. Jaimovich. 2003. IP3 receptors and associated Ca2+ signals localize to satellite cells and to components of the neuromuscular junction in skeletal muscle. *J. Neurosci.* 23:8185–8192.

Rana, Z.A., K. Gundersen, A. Buonanno, and D. Vullhorst. 2005. Imaging transcription in vivo: distinct regulatory effects of fast and slow activity patterns on promoter elements from vertebrate troponin I isoform genes. *J. Physiol.* 562:815–828. doi:10.1113/jphysiol.2004.075333

Rosenblatt, J.D., A.I. Lunt, D.J. Parry, and T.A. Partridge. 1995. Culturing satellite cells from living single muscle fiber explants. *In Vitro Cell. Dev. Biol. Anim.* 31:773–779. doi:10.1007/BF02634119

Roy, R.R., L. Eldridge, K.M. Baldwin, and V.R. Edgerton. 1996. Neural influence on slow muscle properties: inactivity with and without cross-reinnervation. *Muscle Nerve.* 19:707–714. doi:10.1002/(SICI)1097-4598(199606)19:6<707::AID-MUS4>3.0.CO;2-E

Royer, L., S. Pouvreau, and E. Rios. 2008. Evolution and modulation of intracellular calcium release during long-lasting, depleting depolarization in mouse muscle. *J. Physiol.* 586:4609–4629. doi:10.1113/jphysiol.2008.157990

Schiaffino, S., M. Murgia, A.L. Serrano, E. Calabria, and G. Pallafacchina. 1999. How is muscle phenotype controlled by nerve activity? *Ital. J. Neurol. Sci.* 20:409–412.

Serrano, A.L., M. Murgia, G. Pallafacchina, E. Calabria, P. Coniglio, T. Lomo, and S. Schiaffino. 2001. Calcineurin controls nerve activity-dependent specification of slow skeletal muscle fibers but not muscle growth. *Proc. Natl. Acad. Sci. USA.* 98:13108–13113. doi:10.1073/pnas.231148598

Talon, S., C. Huchet-Cadiou, and C. Leoty. 1999. Inositol 1,4,5-trisphosphate-sensitive Ca2+ release in rat fast- and slow-twitch skinned muscle fibres. *Pflugers Arch.* 438:804–816. doi:10.1007/s004240051110

Ursu, D., R.P. Schuhmeier, M. Freichel, V. Flockerzi, and W. Melzer. 2004. Altered inactivation of Ca2+ current and Ca2+ release in mouse muscle fibers deficient in the DHP receptor gamma1 subunit. *J. Gen. Physiol.* 124:605–618. doi:10.1085/jgp.200409168

Valdes, J.A., E. Gaggero, J. Hidalgo, N. Leal, E. Jaimovich, and M.A. Carrasco. 2008. NFAT activation by membrane potential follows a calcium pathway distinct from other activity-related transcription factors in skeletal muscle cells. *Am. J. Physiol. Cell Physiol.* 294:C715–C725. doi:10.1152/ajpcell.00195.2007

Wu, H., S.B. Kanatous, F.A. Thurmond, T. Gallardo, E. Isotani, R. Bassel-Duby, and R.S. Williams. 2002. Regulation of mitochondrial biogenesis in skeletal muscle by CaMK. *Science.* 296:349–352. doi:10.1126/science.1071163

Zafar, S., A. Hussain, Y. Liu, D. Lewis, and G. Inesi. 2008. Specificity of ligand binding to transport sites: Ca2+ binding to the Ca2+ transport ATPase and its dependence on H+ and Mg2+. *Arch. Biochem. Biophys.* 476:87–94. doi:10.1016/j.abb.2008.04.035